AIAA 81-4018

Electronic Damping of Orthogonal Bending Modes in a Cylindrical Mast—Experiment

Robert L. Forward*
Hughes Research Laboratories, Malibu, Calif.

Electronic damping was applied to two orthogonal bending modes in a cylindrical mast. The mast was a 377-g hollow fiberglass cylinder 66 cm long with a 4.3 cm outer diameter and a wall thickness of 0.23 cm. The bottom of the mast was rigidly attached to a large shaker plate, while the top end had a 1500-g inertial mass attached. The two lowest modes of the structure were the two orthogonal first-order bending modes. They had closely spaced resonant frequencies of 33.85 and 34.12 Hz. Although the mechanical Q of each mode was high (500), the modes were just barely separable in a frequency scan. Two orthogonal damping loops were constructed using four small ($25.4 \times 6.35 \times 0.28$ mm) lightweight (0.4 g) piezoelectric ceramic strain transducers as sensors and drivers, the driver for each loop being on the opposite side of the mast from the sensor. The mast mode orientations were not aligned with the damping transducers. Despite the closeness of the modal frequencies and the nonoptimal orientation of the damping loops, a decrease of over 30 dB in the peak amplitudes of the two modes was demonstrated. The behavior of the experimental setup agrees remarkably well with the theoretical predictions of a mathematical model developed by C.J. Swigert in an accompanying paper.

Introduction

ELECTRONIC damping involves the use of electromechanical transducers and electronic feedback loops for the control of mechanical vibrations in structures. Although the concept was studied briefly in the 1950's by Olsen,[1] the technique was forgotten and unused until recently, when it was reinvented[2] for use on large space and optical structures. Sensing transducers are placed on the structure to be damped to detect the dynamic strains or motions induced by the vibrations. The electrical signals from the sensing transducers are amplified and shifted in phase, then reintroduced into driver transducers at some other part of the structure. The driver transducer, acting as a force motor, inserts vibrational energy into the structure so as to produce velocity feedback damping.

In this paper, we demonstrate high levels of damping of two closely spaced bending modes in an end-supported mast. The behavior of the experimental setup as a function of transducer placement, number of damping loops operational, and gain in the damping loops agrees remarkably well with the theoretical predictions of a mathematical model developed by C.J. Swigert.[3]

The sensing transducer is usually a piezoelectric ceramic strain transducer, although resistive and piezoresistive strain gages can be used if the strain levels are high enough. Other sensing transducers that could be used are accelerometers, rate gyros, laser interferometers, and position and angle sensors. In practice, the piezoelectric ceramic strain transducer has proven to be the most effective sensor because of its high sensitivity and ease of application. It has a "gage factor" that is 10,000 to 100,000 times larger than a typical resistive gage,[4] is easily glued to any point on the structure, and presents few weight, volume, or interference problems. When operated into a current amplifier circuit, the voltage at the output of the amplifier is automatically proportional to the rate of change of the strain, simplifying the implementation of a rate damping control loop.

Received Dec. 12, 1979; revision received Aug. 11, 1980.

*Senior Scientist, Exploratory Studies Department. Associate Fellow AIAA.

The driving transducer in the vibration damping loop is usually also a piezoelectric strain transducer, although any type of driver could be used. Other driver transducers that could be used are inertially loaded piezoelectric expanders, voice-coil electromagnetic drivers, torquers, and digitally controlled rotary and linear motors.

Experimental Test Fixture

The mechanical structure used in the experimental work was an omni-antenna mast similar to that used in the Pioneer/Venus spacecraft. It is a hollow fiberglass cylinder with a length of 66 cm, a diameter of 4.3 cm, a wall thickness of 0.23 cm, and a weight of 377 g. It had a 1500 g inertial mass at one end to simulate the antenna mass. The bottom of the mast was firmly attached to a large shake plate (see Fig. 1).

The two lowest modes of the structure were the two orthogonal first-order bending modes, which had closely spaced frequencies of 33.85 and 34.12 Hz. The mast material had very low damping so the bending modes exhibited a sharp, high amplitude response to excitation at the resonant frequency. For such lowly-damped modes a useful parameter called the quality factor, or Q, of the mode is used. One definition of Q is the ratio of the mechanical impedance of the mass of the structure to the damping of the structure ($\omega M/d$). Experimentally the mode Q is best determined from the ratio of the center frequency of the resonant peak to the half-power bandwidth of the resonance ($f/\Delta f$). Although the mechanical Q of each mode was high (480 and 510), the modes were so close in frequency they were just barely separable in a frequency scan.

At a point 6.5 cm from the base of the mast were placed four piezoelectric ceramic strain transducers. The four transducers were operated in parallel as a driver array to excite vibrations in the two modes.

At a point 15 cm from the bottom of the mast, two orthogonal damping loops were constructed using two sets of single transducers (see schematic in Fig. 2). One transducer was used as a pickoff to sense the dynamic strains in the mast, and the transducer on the opposite side was used as the force driver for the feedback loop. As it turned out, the vibrational axes defined by the two orthogonal mechanical modes in the experimental apparatus were at 51 deg to the damping axes defined by the transducers in the damping loops, and hence

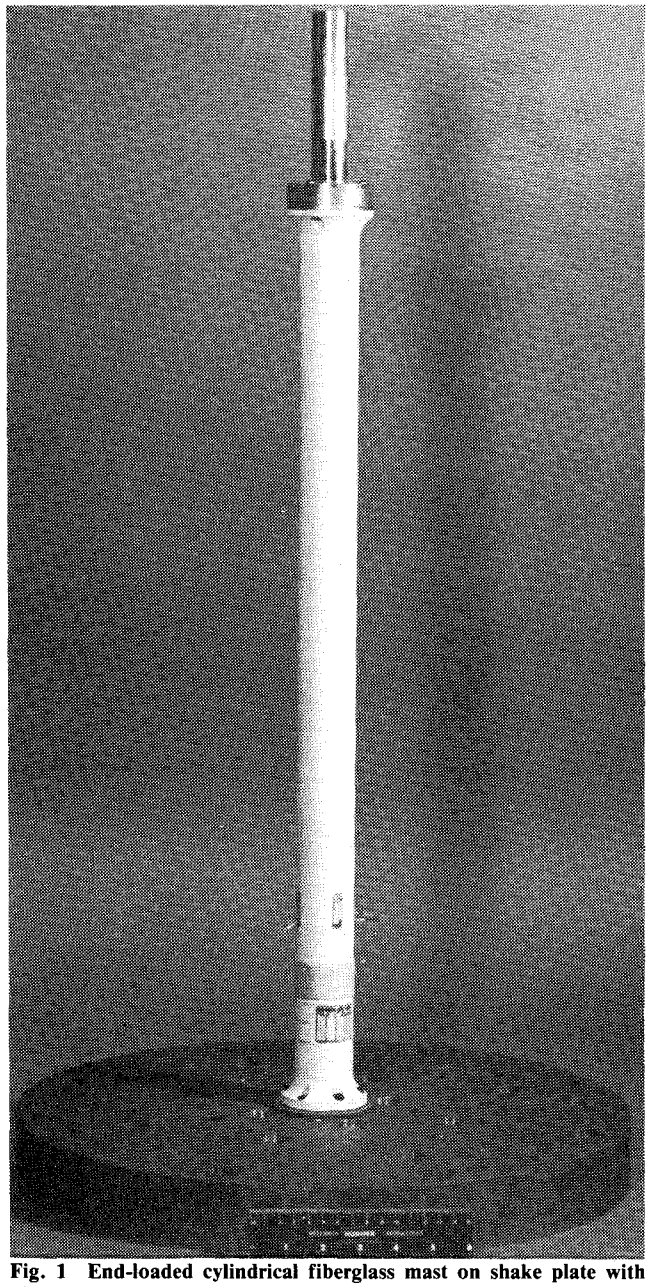

Fig. 1 End-loaded cylindrical fiberglass mast on shake plate with piezoelectric ceramic strain transducers attached.

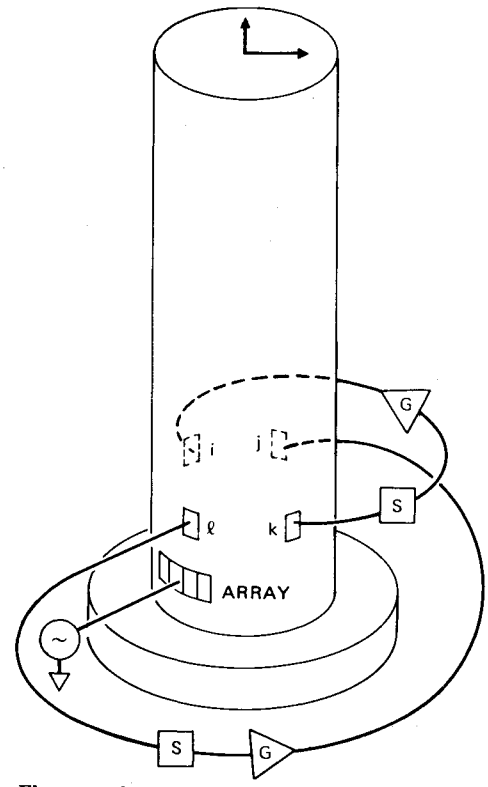

Fig. 2 Electromechanical schematic of mast showing relative orientation of four-transducer driver array, sensing, and driving transducers in feedback damping loops and mast vibrational modes.

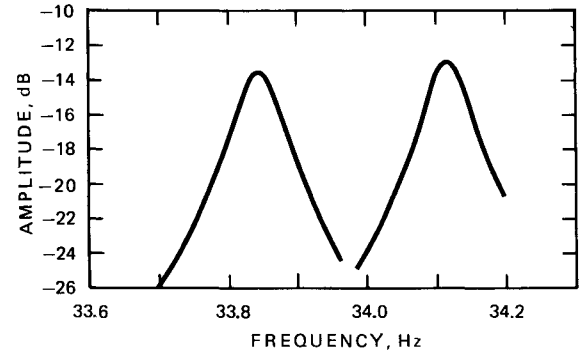

Fig. 3 Expanded frequency scan of both mast modes using drive voltages that would excite each mode independently.

there was nearly equal coupling from each transducer into both modes.

The piezoelectric transducers used in our electronic damping work were usually Gulton SC-4 (now superceded by SG-4M) strain transducers with a size of $25.4 \times 6.35 \times 0.25$ mm ($1.0 \times 0.25 \times 0.01$ in.) and a nominal capacity of 4700 pF. These transducers weigh only 0.4 g, yet four of them weighing a total of 1.6 g can damp a 377 g mast loaded with a 1500-g inertial weight. The SG-4M transducers are convenient because they come supplied with leads. We use them both as strain sensors and motor drivers. These transducers have an excellent electrical-to-mechanical coupling and a voltage sensitivity to strain that is 50,000 times that of a resistive wire strain gage.[4]

Since the two bending modes of the mast were very close together, it was difficult to measure their quality factor or Q separately. But since the two modes are orthogonal in spatial orientation, directional excitation can be used to make separate measurements on each mode.

The frequency and Q of the individual modes were determined by driving two adjacent damping transducers in parallel and combining the outputs of the other two damping transducers. Since the mode orientation of 51 deg was close to 45 deg, this sufficed to obtain a clean measurement of each mode separately. (If the modes are not near 45 or 0 deg, then different levels of drive to two adjacent transducers would provide the proper single-mode excitation.)

As shown in Fig. 3, the modes were separable, and careful measurement of the center frequency and the half-power (3 dB) bandwidth produced the modal properties shown in Table 1.

Table 1 Mode parameters

	Frequency	Q
Upper mode	34.12	510
Lower mode	33.85	480

Relative Transducer Coupling

When the driver array was excited by the reference voltage from a frequency response analyzer with the electronic damping circuits inactive, we could measure the transfer function from the driving array to each of the four damping transducers. Typical response curves are shown in Fig. 4. They show that the driving transducer was about equally coupled into the first two bending modes of the mast at about 33.85 and 34.12 Hz. The sharp dip between the modes in Figs. 4(*ℓ*) and 4(*k*) is a zero in the response caused by interference between the two orthogonal modes. They are being driven in phase for that sensor by the driver array. At that excitation frequency, one of the modes is being driven above resonance and its respone has shifted 180 deg, while the other is still being driven below resonance and so its response is in phase with the driving force. The two responses tend to cancel each other at this frequency, producing the zero. In Figs. 4(*j*) and 4(*i*) the two responses are in phase and add.

We next measured the transfer function between the various pairs of damping transducers to determine the transducer-to-transducer coupling coefficients that would affect the performance of a feedback loop using that pair of transducers. These are shown in Fig. 5, where we used only one of each pair of transfer functions. The power transfer function between any pair of transducers should, because of energy reciprocity laws, be the same when the driver and sensor roles of the two transducers are reversed. However, these traces are voltage transfer functions, and there were minor differences

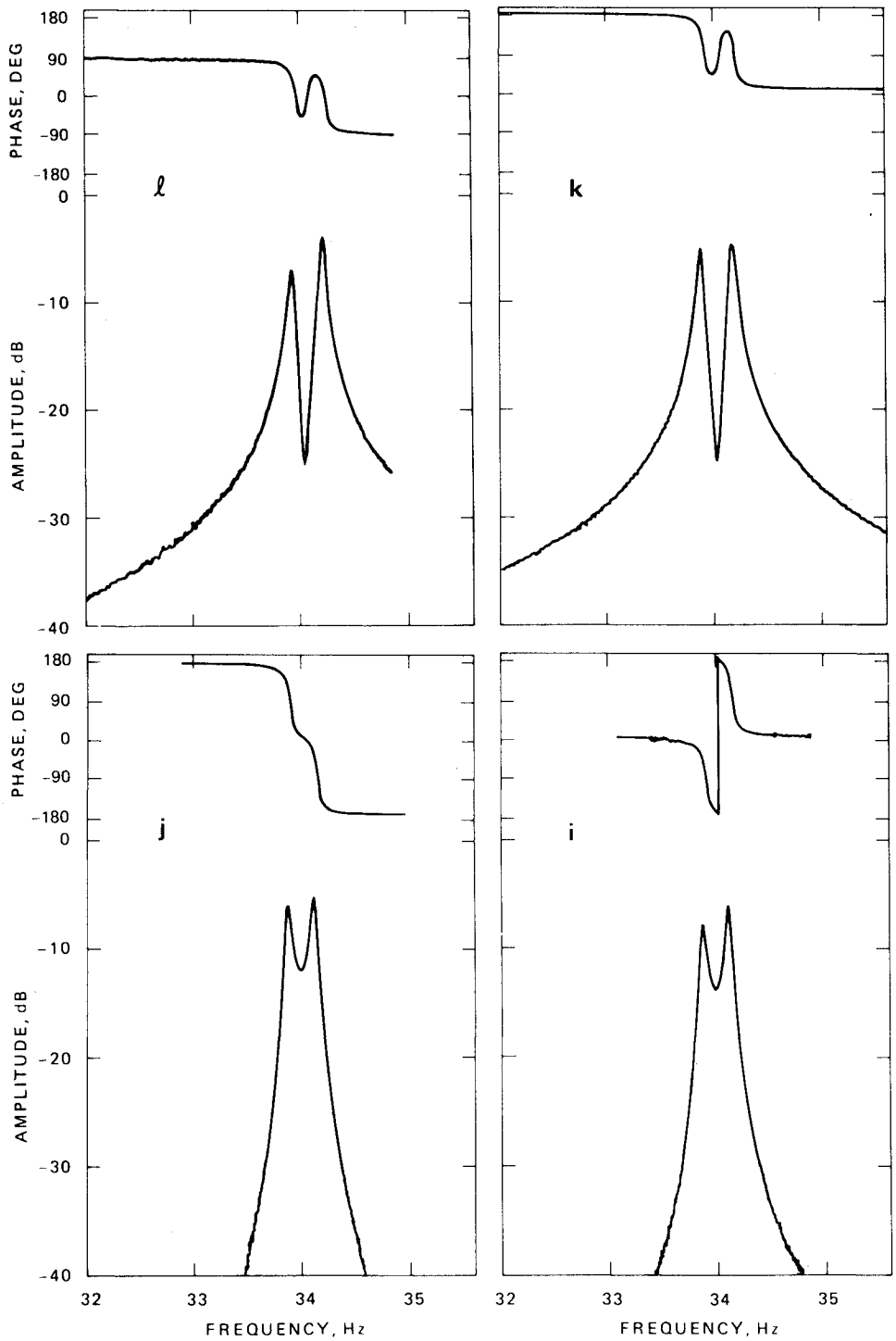

Fig. 4 Phase and amplitude voltage transfer functions from the driver array to each of the four damping tansducers.

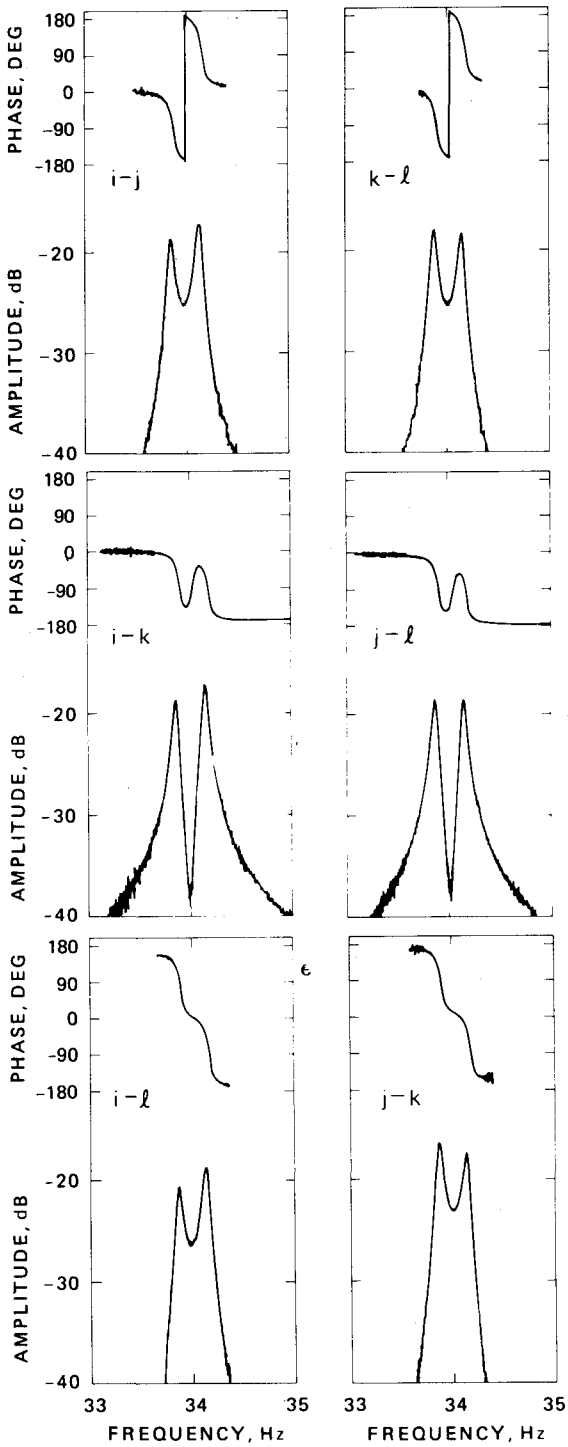

Fig. 5 Phase and amplitude voltage transfer functions between the four damping transducers.

between the transfer functions measured in opposite directions, due to slight differences in the capacitance and leakage resistance of the transducers.

The data taken from these transfer functions were then combined to give an estimate of the relative coupling of each transducer to the mast (see Table 2). These are all essentially the same. Relative to the damping transducers, the driving array had a coupling of 5.32. These coupling coefficients were later used in the computer simulation carried out in the accompanying paper.

Electronic Damping Circuits

The damping circuits used in the experimental apparatus were laboratory prototypes with a great deal of adjustability in phase and amplitude to simplify laboratory procedures. The signal conditioning circuits consisted of a zero-input-impedance operational amplifier circuit that converted the current coming from the capacitive transducers into a voltage (thus automatically introducing a 90 deg phase shift). The preamplifier was followed by a bandpass filter peaked at the resonant frequency of the modes, a phase shifter capable of nearly 360 deg of phase shift, and a final high-voltage (±150-V) amplifier-driver. The preamplifier/filter/phase-shifter circuit is shown in Fig. 6. The circuit has the nice feature that it can be separately adjusted in frequency, gain, phase, and Q with minimum "crosstalk" between the various parameters. In actual system operation, this circuit can probably be replaced with the preamplifier, a simple nonadjustable filter, and a power stage appropriate to the vibration amplitudes that the damping circuit must handle. If the undamped vibration levels in the structure are not so high as to induce visible motion in the structure, then the ±15 V output of the filter will probably be sufficient for damping. Otherwise, a final high-voltage stage will be needed.

Table 2 Transducer coupling parameters

Transducer	Relative coupling
i	0.90
j	1.09
k	1.06
ℓ	0.95

For the experimental work, the filters were set near the two resonant frequencies of the two modes, the Q was set to be fairly broad (a Q of 11, or a bandwidth of 3.1 Hz), and the phase was adjusted a few degrees to give optimum damping. When the circuit is loaded with a piezoelectric ceramic transducer, an additional 90 deg phase shift is introduced, producing an output voltage suitable for velocity feedback damping when applied to the feedback transducer.

Single Damping Loop Experiments

We first hooked up one of the two orthogonal damping circuits to study the effect of a single feedback damping loop on the two mast modes. We used one of the damping transducers as the sensing element and the damping transducer on the opposite side of the mast as the driver. Since the two modes were both about equally coupled into both of these transducers, we hoped that a single damping loop would suffice to damp both modes. (This turned out to be only partially true.) To monitor the effect of the feedback damping loops on the modes, we drove the array of four transducers with a swept-frequency signal and monitored the output of the various damping transducers (except the one being used as the driver in the feedback loop).

In the first experimental setup, the feedback loop used the ℓ transducer as the sensor and the j transducer as the driver. The feedback gain was increased in increments, and a transfer function between the array and the ℓ transducer was measured. This is shown in Fig. 7. With increasing feedback gain, both modes are about equally damped, and, at a feedback gain of +20 dB, the modes are completely damped. The "bump" at 32 Hz and the rising trend at 35 Hz are due to the finite bandwidth of the filter. The phase shift in the skirts of the filter is not optimal for damping, and, at very high feedback gains, there is actually a bit of amplification starting, even though the center is highly damped. Also note in Fig. 7 that, although both modes appeared to be highly damped by a single feedback damping loop, the damping loop did not seem to have any effect on the zero.

Keeping the feedback circuit operating between the j and ℓ transducers, we then measured the transfer function between the driving array and the k transducer (see Fig. 8). Here again,

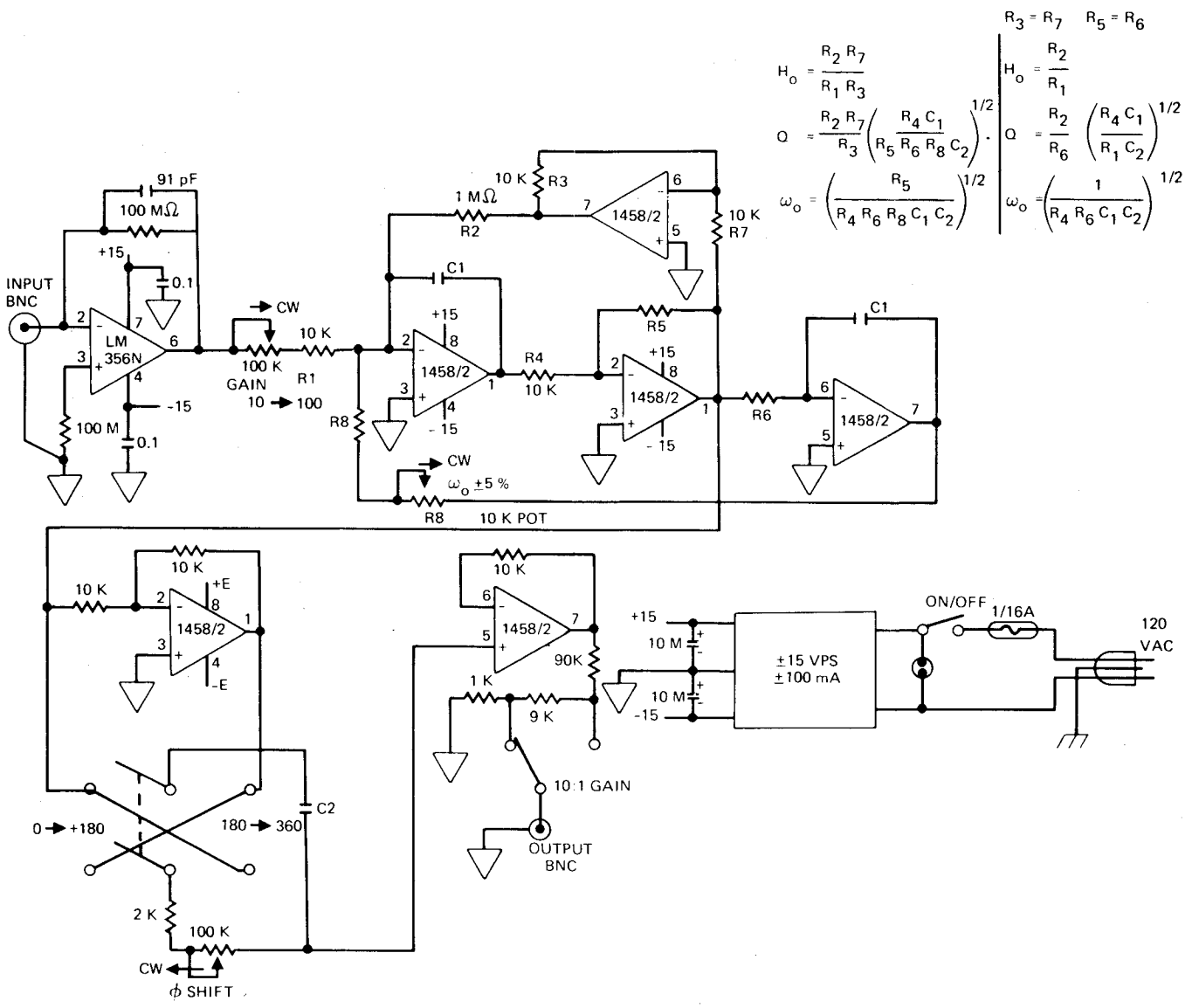

Fig. 6 Schematic of preamplifier/filter/phase-shifter circuit.

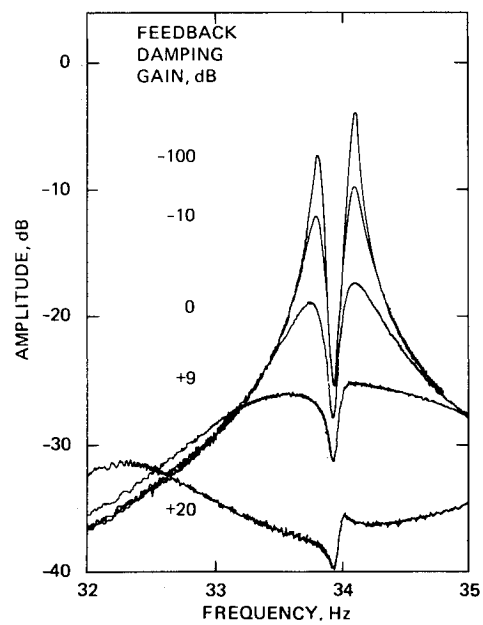

Fig. 7 Amplitude transfer function between array and the ℓ transducer as a function of feedback gain in ℓ-j damping loop.

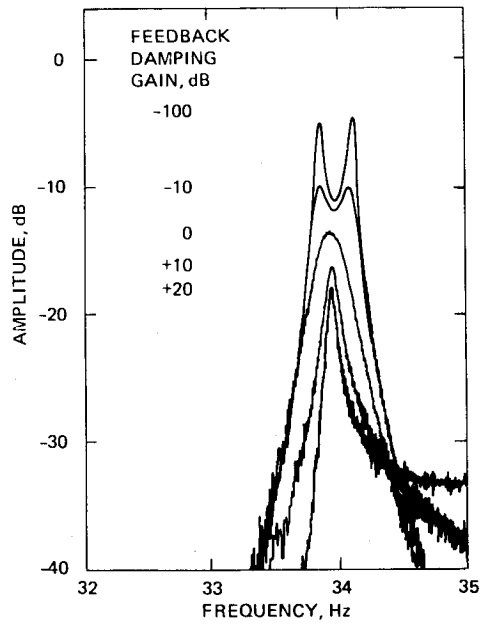

Fig. 8 Amplitude transfer function between array and k transducer as a function of feedback gain in ℓ-j damping loop.

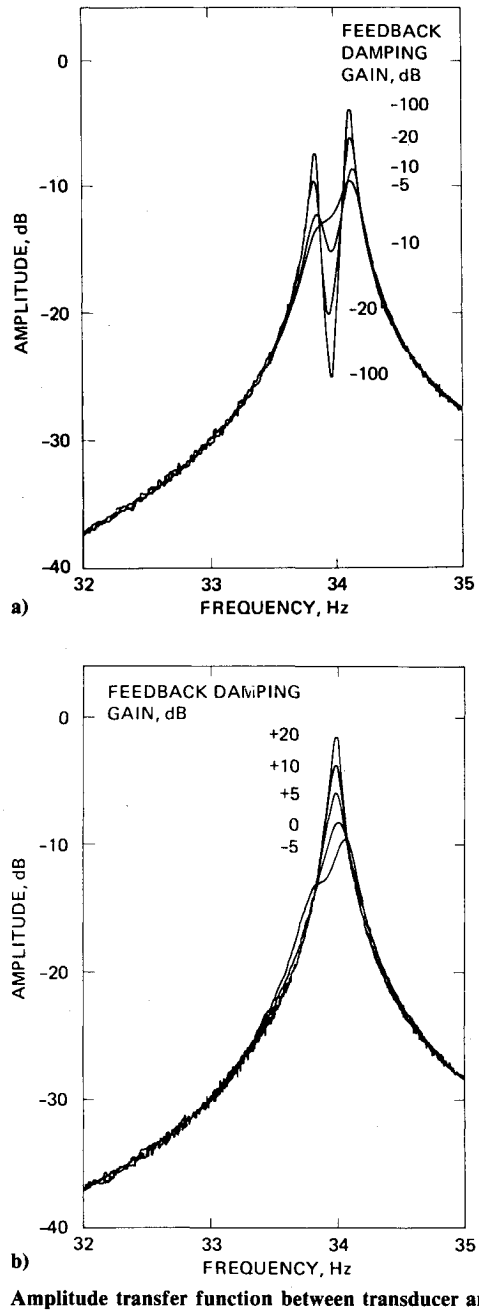

Fig. 9 Amplitude transfer function between transducer array and *j* transducer as a function of feedback gain in *k-i* damping loop: a) low feedback gains, b) high feedback gains.

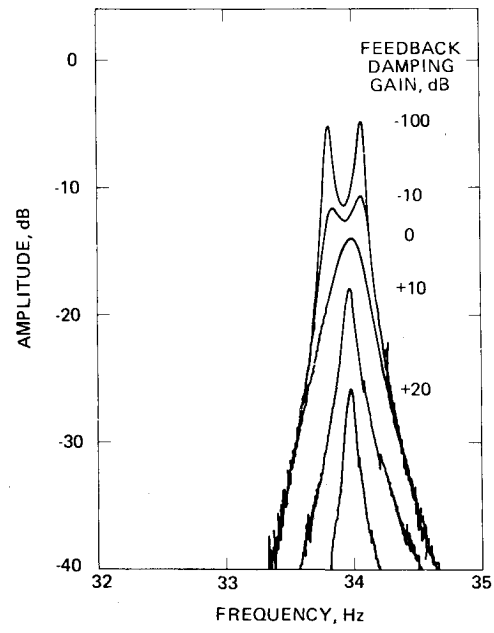

Fig. 10 Amplitude transfer function between transducer array and *k* transducer as a function of feedback gain in *k-i* damping loop.

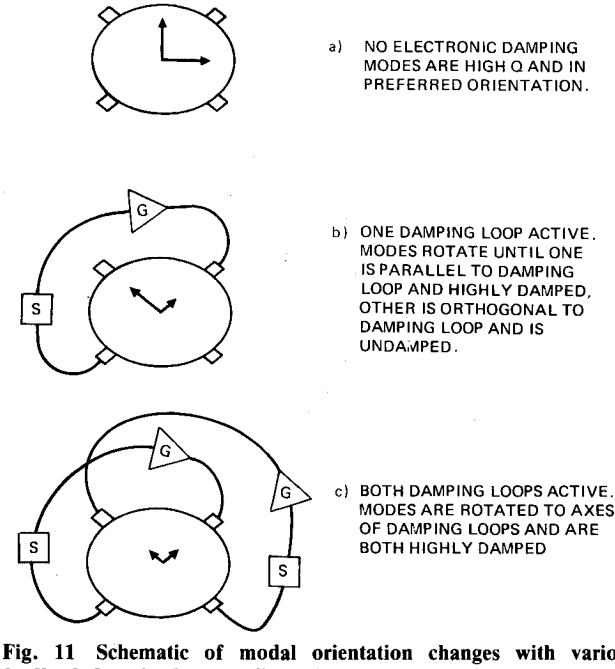

Fig. 11 Schematic of modal orientation changes with various feedback damping loop configurations.

the two mast modes are broadening and decreasing in amplitude and combining into a single damped mode as the feedback gain is increased. Yet, as the gain is made higher, something strange occurs. The amplitude of the combined mode becomes smaller, but the mode shape becomes sharper, as if the mode were becoming a high-Q mode again. Yet, if the mode Q were increasing, the amplitude response of the mode to the constant amplitude driving forces from the array should be increasing.

We then switched the feedback damping loop to the orthogonal pair of damping transducers. The *k* transducer was used as the sensor and the *i* transducer was used as the driver. We again excited the mast modes with the transducer array and measured the transfer function from the array to the *j* transducer. As Fig. 9a shows, the *k-i* feedback loop not only damps both of the mode resonances, it also damps the zero. As the feedback gain is increased, the two modes and the zero start to mold into a single, slightly humped, damped mode. However, the amplitude of the combined mode is not dropping as fast as it did in Fig. 8.

We then increased the feedback gain even further. As we see in Fig. 9b, this *decreased* the damping of the mode. Finally, at +20 dB (the highest damping practical with the experimental apparatus), we find not two modes but a single mode with a Q that has almost returned to the undamped Q of the original modes and a frequency that is between the two resonant frequencies of the original mast modes.

We then look at what is happening in the orthogonal direction by measuring the transfer function between the array and the *k* transducer. As the feedback gain is increased, we first see damping and broadening of the two mast modes until they have combined into one broadened mode (see Fig. 10). With increasing gain, the combined mode continues to shrink in amplitude, but again it sharpens until it has almost reached the high-Q state possessed by the original modes.

The interpretation of the preceding experiments is shown in Fig. 11. When the damping loops are inactive, the orthogonal

modes of the mast have a high Q and are in their preferred orientation, as determined by the minor variations in the shape and elasticity of the nominally cylindrically symmetric mast (see Fig. 11a). In our apparatus, the mode coordinate axes were at 51 deg to the transducer coordinate axes. With one damping loop active, the modes are, at first, both damped in proportion to the amount of coupling to the damping loop. In addition, as shown in Fig. 11b, the damping loop causes a "rotation" of the modal axes. The mode closest to the damping loop is pulled into alignment with the damping loop and becomes more highly damped, while the orthogonal mode rotates until it becomes orthogonal to the damping loop axis. The coupling to the damping loop drops because of the decreasing angular coupling, and the damping of that mode actually decreases with increased feedback gain.

The rotation of the modes can be interpreted in either of two ways, both of which are probably equivalent ways of describing the same effect. The rotation could be thought of as a physical rotation of the modes to line up with the preferred axes of the structure, with the feedback damping loop causing a change in the combined electromechanical properties of the mast. Alternatively, the rotation could be thought of as a linear recombination of the original modes into a new orthogonal set under the influence of the feedback damping loop.

In our experimental setup, the driving transducer array was in the same angular position as the ℓ transducer and 8.5 cm lower on the mast. Thus, when the ℓ-j feedback loop was operational, the mode that was rotating to be orthogonal to the damping loop was also rotating away from the driving array, decreasing the amount of drive coupled into that mode from the driving array. This decoupling by rotation more than compensated for the increased coupling due to the increasing Q of the mode.

As is shown later, if both feedback loops are operational, the modes will rotate as shown in Fig. 11c until they are aligned with the feedback damping loops and have become highly damped.

Double Damping Loop Experiments

We then activated both feedback damping loops. One was arranged with transducer ℓ as the sensor and transducer j, on the opposite side of the mast, as the driver. The orthogonal damping loop used transducer k as the sensor and i as the driver. We first measured the transfer function from the array to the ℓ transducer. The data for various levels of feedback gain are shown in Fig. 12 (ℓ). We repeated the measurements in the orthogonal direction by measuring the transfer function from the array to the k transducer. These results are shown in Fig. 12(k): both modes are damped with increasing feedback gain in the damping loops, the peak amplitude drops by 30 dB or more, and there is no evidence of any high-Q mode having "escaped" the influence of the damping loops.

The decrease in amplitude in Fig. 12(k) with increasing feedback gain is faster than it is in Fig. 12(ℓ). This occurs because, in Fig. 12(ℓ), the two modal responses are in phase, since the sensing transducer ℓ is along the same axis as the driving array. Thus, as the two modes broaden and overlap, they reinforce each other. In Fig. 12(k), the sensing transducer, being orthogonal to the driving array, senses one mode in phase with the driving voltage and the other mode 180 deg out of phase. When the modes broaden and overlap, they partially cancel each other, causing a more rapid decrease in response amplitude with increasing feedback gain.

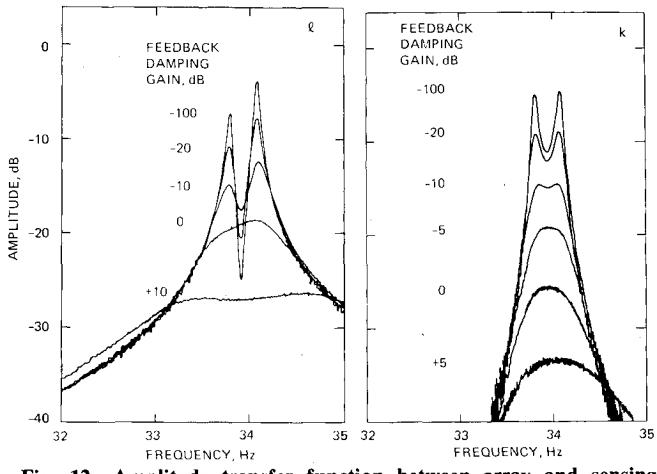

Fig. 12 Amplitude transfer function between array and sensing transducer ℓ and k as a function of equal feedback gain in both damping loops.

Conclusions

Using electronic feedback between two pairs of orthogonally disposed piezoelectric transducers, we have demonstrated high levels of damping of two orthogonal vibrational bending modes in a cylindrical mast. The modes were closely spaced in frequency (33.85 and 34.12 Hz) and were not preferentially aligned with the electronic damping loops. The transducers, although small ($25.4 \times 6.35 \times 0.28$ mm) and light (0.4 g), were able to achieve high levels of damping (>30 dB) in both modes of the heavy (377 g), inertially loaded (1500 g), rigid fiberglass mast. We also showed that a single damping loop can produce some damping in both modes at low feedback gain, but that higher gains only produce high damping in one mode, while the other mode shifts in frequency, rotates in orientation, and returns to its original Q. The data obtained in the experimental work agree remarkably well with the theoretical predictions of a mathematical model of the combined electromechanical system developed by C.J. Swigert in an accompanying paper.

References

[1] Olsen, H.F., "Electronic Control of Noise, Vibration, and Reverberation," *Journal Acoustical Society,* Vol. 28, Sept. 1956, pp. 966-972.

[2] Forward, R.L., "Electronic Damping of Vibrations in Optical Structures," *Applied Optics,* Vol. 18, March 1979, pp. 690-697.

[3] Swigert, C.J. and Forward, R.L., "Electronic Damping of Orthogonal Bending Modes in a Cylindrical Mast—Theory," *Journal of Spacecraft and Rockets,* Vol. 18, Jan.-Feb. 1981.

[4] Forward, R.L., "Picostrain Measurements with Piezoelectric Transducers," to appear in *Journal of Applied Physics,* Jan. 1981.